

## CHAPTER 33

# SIMULATION OF EL NIÑO OF 1982-1983

S.G.H. PHILANDER and A.D. SEIGEL

## ABSTRACT

A general circulation model of the ocean simulates El Niño of 1982-1983 with reasonable success and provides the following results. The massive eastward transfer of warm surface waters from the western to the eastern Pacific was accomplished by unusual eastward surface currents which, by November 1982, extended from 9°S to 9°N across 120°W. Further east, the persistence of the south-east trades over the eastern tropical Pacific inhibited eastward surface flow at, and to the south of the equator at that time, but the eastward flow between 3° and 8°N penetrated right to the coast of Central America. The relaxation of the trades and the changes in the curl of the windstress, that caused the redistribution of heat in the upper ocean, occurred so gradually between June and November 1982 that the response of the ocean was approximately an equilibrium one. The zonal pressure gradient along the equator and the intensity of the Equatorial Undercurrent, for example, decreased gradually as the trade winds weakened. In December 1982, the anomalous eastward winds west of the dateline suddenly changed to northerly winds. The westward pressure force which the eastward winds had established was left unbalanced. This excited an eastward travelling equatorial Kelvin wave which elevated the thermocline and accelerated the equatorial currents westward. The wave front dispersed downwards as it propagated eastward and there is no evidence of its reflection at the South American coast affecting the surface layers of the ocean. Eastward winds in the eastern equatorial Pacific Ocean in March and April interrupted the recovery from El Niño and generated an intense local eastward surface jet. The reappearance of the tradewinds in May 1983 signalled the end of El Niño and the gradual return to normal conditions.

## INTRODUCTION

Though El Niño of 1982-1983 is far better documented than any previous El Niño, the available data are too fragmented to provide a complete picture of the development of this El Niño. Simulation of El Niño therefore serves two purposes. It is a test of the realism of the model and, should the model be reasonably successful in reproducing the available measurements, then the model results from regions where data are unavailable can be used to paint a coherent picture of the evolution of the event. This paper describes a simulation of El Niño of 1982-1983 with a general circulation model of the tropical Pacific Ocean. Unfortunately, the winds used to drive the model - 1000 mb monthly mean winds provided by the National Meteorological Center - are known to have flaws (E. Rasmusson and J. O'Brien, pers. commun., 1984). It is, therefore, unclear whether discrepancies between the measurements and the results from the model are attributable to the poor wind data, or to deficiencies of the model. The same model has performed successfully in a simulation of the well-documented seasonal cycle of the tropical Atlantic Ocean (Philander and Pacanowski, 1984; Katz, 1984). We are therefore inclined to attribute discrepancies between the model's results and the measurements primarily to

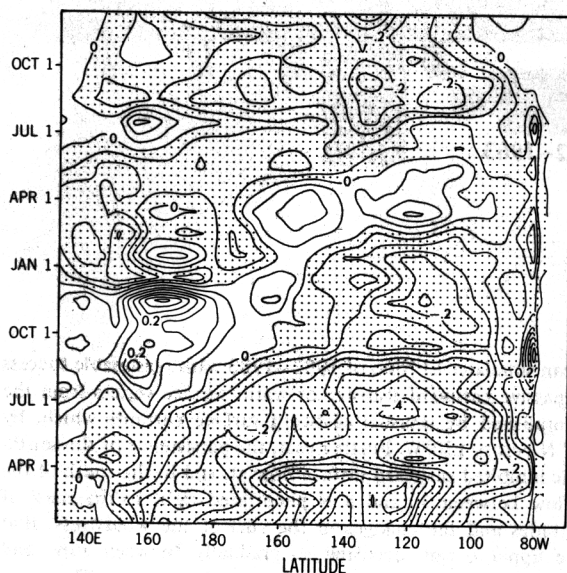


Fig. 1. Zonal wind stresses averaged between  $5^{\circ}\text{N}$ – $5^{\circ}\text{S}$  for 1982–1983. Shading represents westward direction. Contour interval is  $0.05 \text{ dynes cm}^{-2}$ .

inaccuracies in the wind fields. These discrepancies are fortunately not too serious, so that the results from the model can be used to obtain a coherent picture of how El Niño developed.

This paper is organized as follows: Section 2 describes the winds that force the model, and briefly summarizes the measurements obtained in 1982 and 1983; Section 3 is a description of the model; Section 4 is a presentation of the results; and Section 5 is a summary.

## 2. THE MEASUREMENTS

El Niño of 1982–1983 evolved in three stages: Up to November 1982, there was a relaxation of the trade winds that led to the appearance of eastward winds west of the dateline; between December 1982 and May 1983, the winds over the western Pacific were cross-equatorial and had only a small zonal component near the equator, while the easterly winds over the eastern Pacific weakened and became westerly; the final stage of the event started in May 1983 with the return of the tradewinds, first in the central Pacific, then elsewhere. These changes are evident in Figs. 1–3.

The relaxation of the trade winds during the first phase of El Niño resulted in a massive transfer of warm surface waters from the western to the eastern tropical Pacific Ocean. The available measurements give an incomplete picture of how this occurred. Sea-level measurements (Wyrski, 1984a, b) reveal that the thermocline first started to rise in the region west of the dateline, between the equator and  $15^{\circ}\text{N}$  approximately. During the subsequent months (until December 1982) this region in which the thermocline shoaled, expanded eastward to about  $160^{\circ}\text{W}$ , and also expanded southward across the equator. Geostrophic calculations based on XBT data from tracks between New

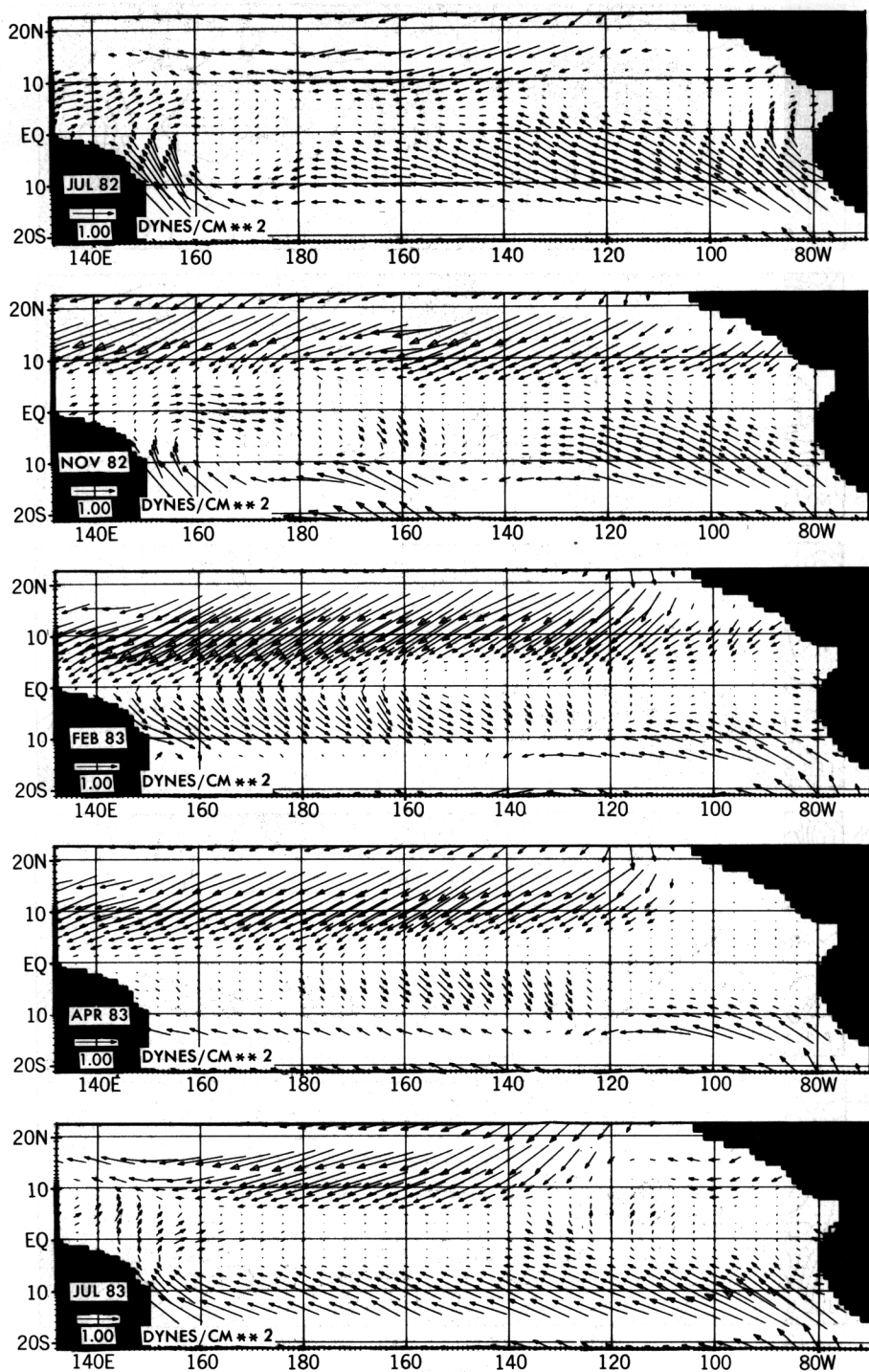


Fig. 2. 1000 mb NMC monthly averaged wind stresses used to force the model.

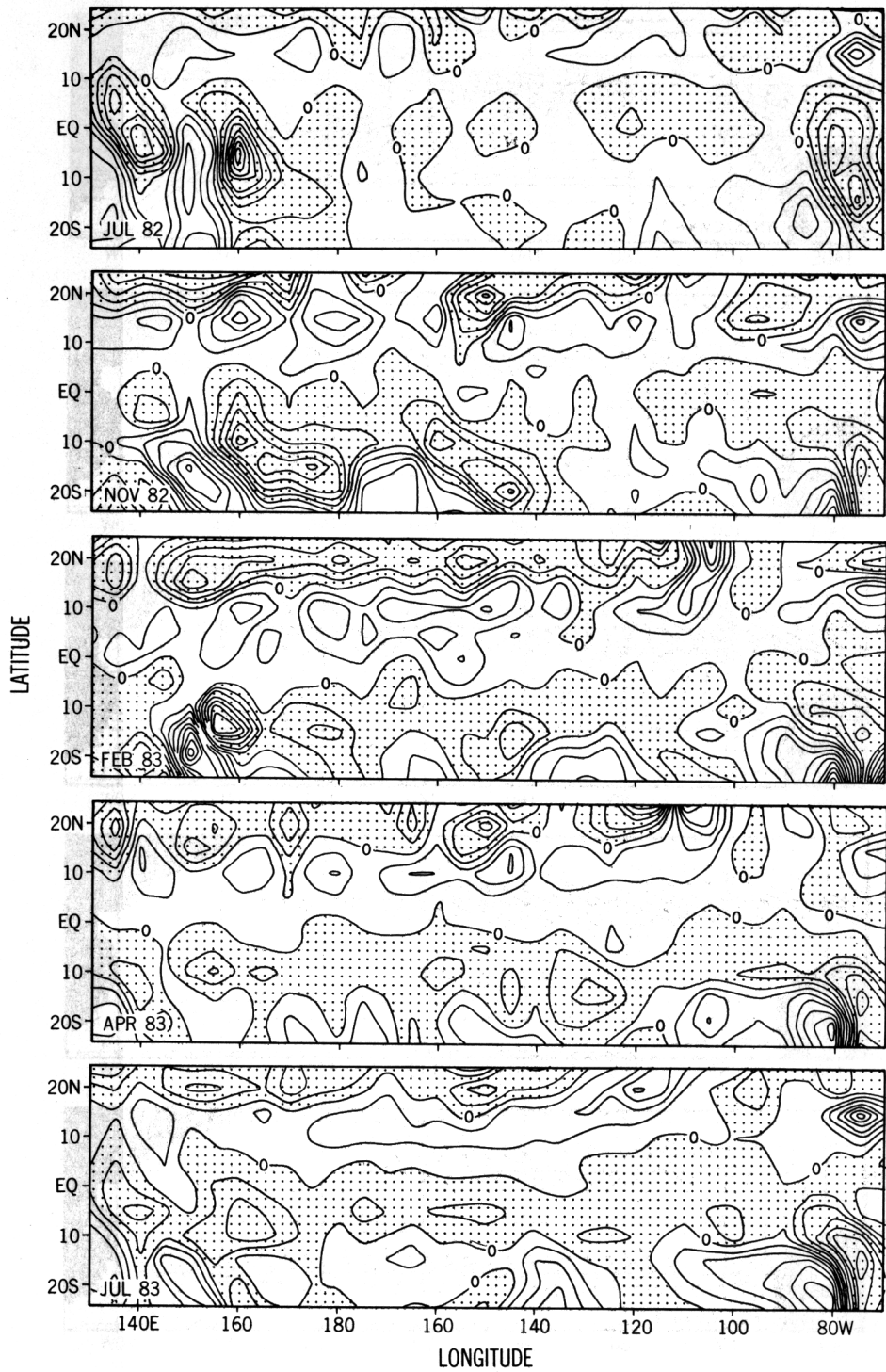


Fig. 3. Curl of the wind stresses for different months before interpolation to the model resolution. Contour interval is  $1.0 \times 10^{-8}$  dynes  $\text{cm}^{-3}$ . The curl is negative in shaded areas.



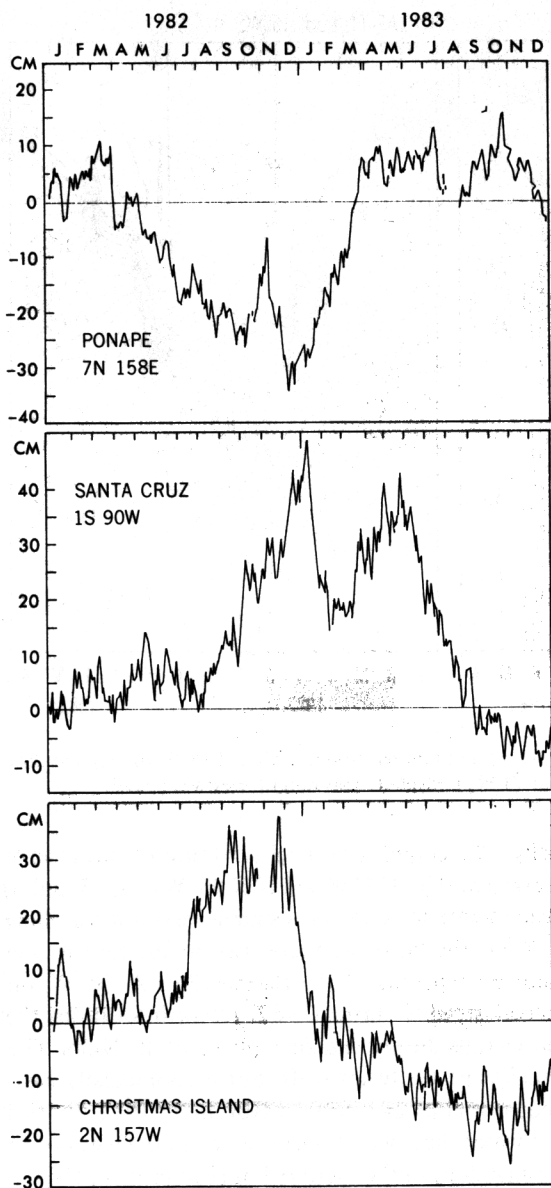


Fig. 4. Observed sea level at various locations in the Pacific (after Wyrtki, 1984a).

Caledonia and Japan (Meyers and Donguy, 1984) and between New Zealand and California (Kessler, pers. commun., 1984) show that an intensification of the North Equatorial Countercurrent (between  $3^{\circ}$  and  $9^{\circ}\text{N}$  approximately) transferred the warm surface waters eastward as the thermocline in the west rose. (Direct current measurements are unavailable for the region west of  $160^{\circ}\text{W}$ .) Sea-level measurements at different meridians document the eastward march of the increase in heat content of the water column. In Fig. 4, the increase in sea level at Christmas Island is seen to precede that

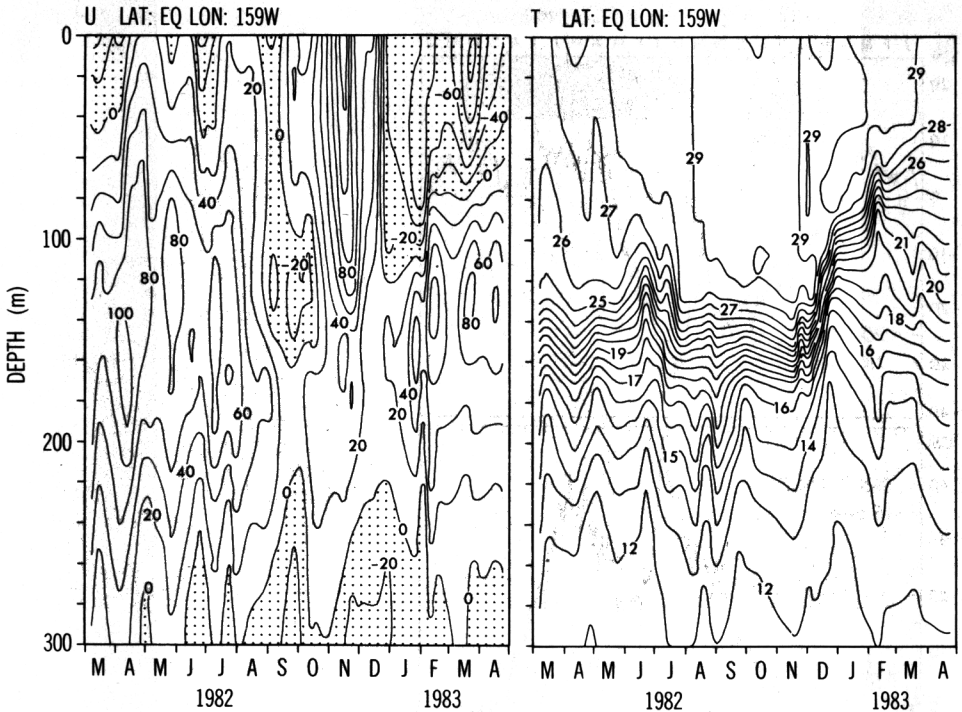


Fig. 5. The observed zonal velocity fields ( $\text{cm s}^{-1}$ ) and temperature (in  $^{\circ}\text{C}$ ) at  $159^{\circ}\text{W}$  and the equator during 1982–1983 as measured by Firing et al. (1983). Shaded areas denote westward flow.

at the Galapagos Islands by several weeks. The complex vertical structure of this change in the heat content of the ocean, as observed at  $0^{\circ}\text{N } 159^{\circ}\text{W}$  and  $0^{\circ}\text{N } 95^{\circ}\text{W}$  (Figs. 5 and 6) precludes an interpretation of the measurements in terms of a simple eastward travelling vertical mode of the ocean. At  $159^{\circ}\text{W}$  on the equator, there was an increase in the temperature of the surface layers but not a deepening of the thermocline. At  $95^{\circ}\text{W}$ , on the other hand, the thermocline deepened steadily during 1982. At both locations the Equatorial Undercurrent is seen to decelerate during the first phase of El Niño. The flow in the surface layers is not the usual swift westward drift, but is sporadically eastward and includes an intense eastward equatorial jet at  $159^{\circ}\text{W}$  in November 1982. By this time, a sufficient amount of warm surface waters had been transferred from the western to the eastern Pacific to eliminate the usual zonal slope of the thermocline (Firing et al., 1983).

The second phase in the development of El Niño starts in December 1982 with the deceleration of the eastward equatorial jet at  $159^{\circ}\text{W}$ . This coincided with a rise of the thermocline and a fall in sea level. In the western Pacific to the south of the equator, sea level dropped steadily during the next six months (Wyrtki, 1984a) but in the eastern Pacific, developments were more complex. At first, in January and February 1983, sea level fell, the thermocline shoaled, the Equatorial Undercurrent disappeared and the surface flow was westward (Fig. 6; Hansen, 1984). In April and May, however, sea level rose again because of an increase in sea-surface temperature rather than a deepening of

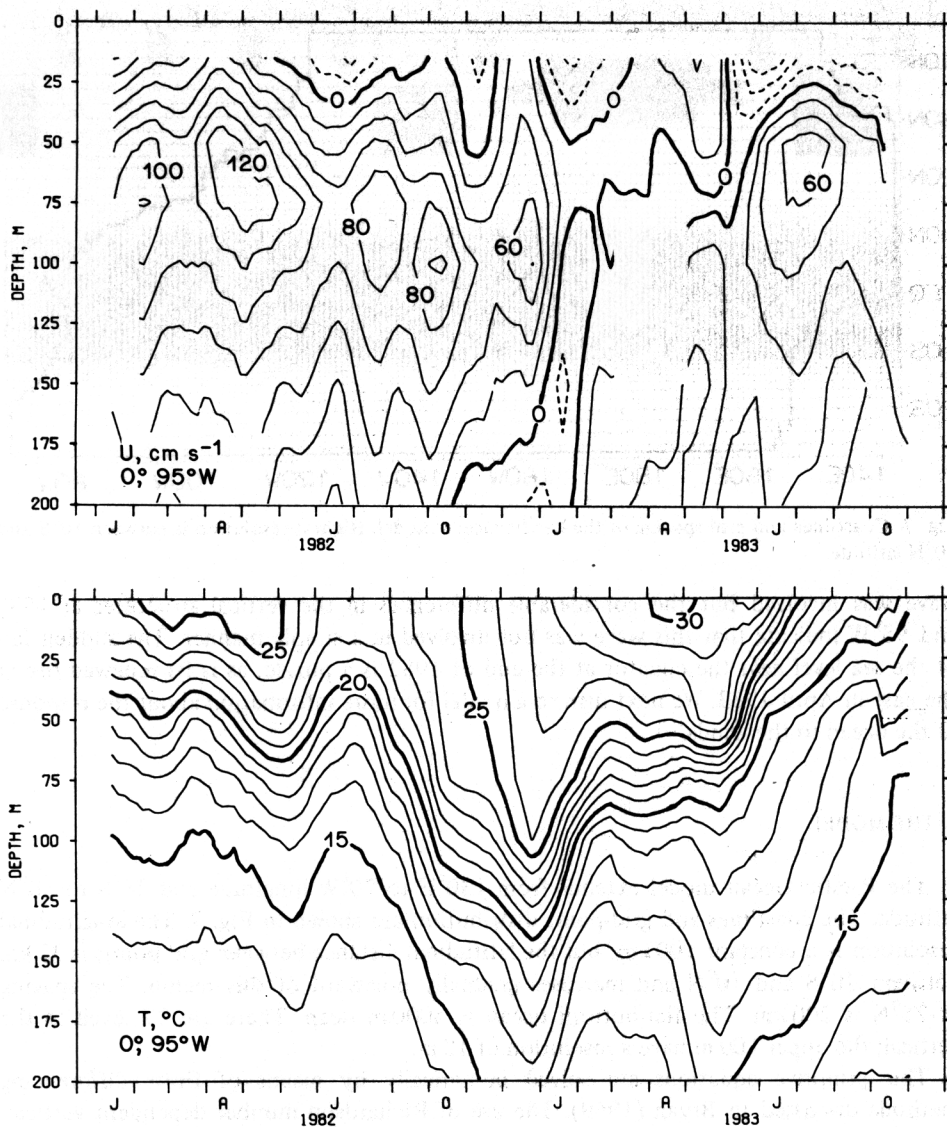


Fig. 6. The observed zonal velocity fields and temperature at  $95^{\circ}\text{W}$  and the equator during 1982–1983 as measured by Halpern (1984). Dashed contours indicate westward flow.

the thermocline (Fig. 6), and an eastward jet appeared in the surface layers. Finally, in June 1983, the return of the trade winds started the restoration of normal conditions.

The oceanic changes during El Niño are in response to the changes in the surface winds but with the available measurements it is impossible to establish which wind variations caused specific changes in the ocean. The relaxation of the tradewinds during the first phase of the event presumably resulted in the eastward transfer of heat in the upper ocean, but the pattern of currents that effected this redistribution is unclear. The eastward phase propagation of the rise in sea level near the equator suggests that a Kelvin

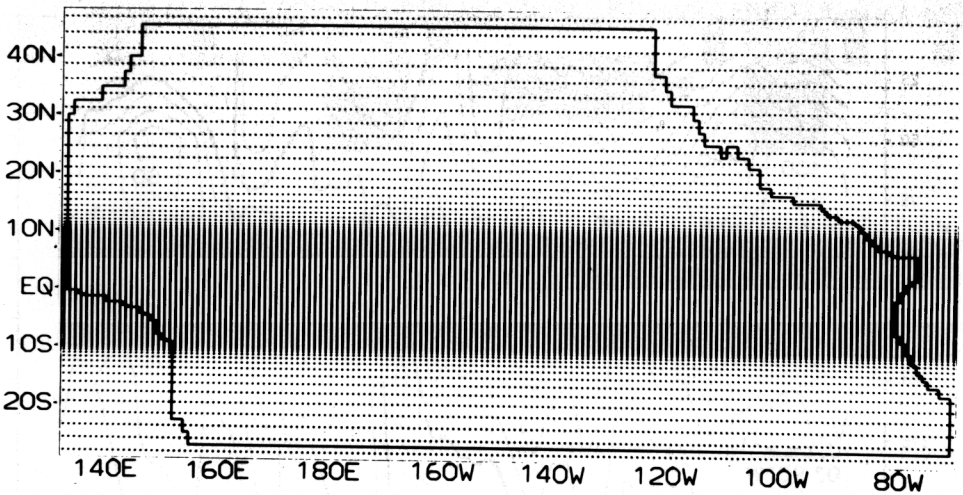


Fig. 7. Coastlines and grid-spacing of the Pacific Ocean model. Highest resolution is between 10°S and 10°N latitude.

wave was involved but the considerable differences in the vertical structures at 159° and 95°W indicate that this wave was not involved in a simple manner. The sudden fall of the sea level near the equator at the end of 1982 is a puzzle, as is its renewed rise in the east in April 1983. We next turn to a model for more information about the response of the ocean to the winds.

### 3. THE MODEL

The Pacific Ocean model extends from 130°E to 70°W longitude and 28°S to 50°N latitude. The coastlines and grid-point distribution are shown in Fig. 7. The longitudinal resolution is a constant 100 km, but the latitudinal distance between grid points is 33 km between 10°S and 10°N and increases gradually poleward of this region. The spacing at 25°N is 200 km. The flat-bottom ocean is 4000 m deep. There are 27 levels in the vertical; the upper 100 m have a resolution of 10 m.

The primitive equations are solved numerically by means of finite differencing methods discussed in Bryan (1969). The use of Richardson number dependent vertical-mixing coefficients is explained in detail in Pacanowski and Philander (1981). The coefficient of vertical eddy viscosity is assigned a constant value of  $10 \text{ cm}^2 \text{ s}^{-1}$  in the upper 10 m of the model to compensate for mixing by the high-frequency wind fluctuations which are absent from the monthly mean winds. The coefficient of horizontal eddy viscosity has the constant coefficient  $2 \times 10^7 \text{ cm}^2 \text{ s}^{-1}$  equatorward of 10° latitude and elsewhere varies inversely as the latitudinal resolution to a value of  $50 \times 10^7 \text{ cm}^2 \text{ s}^{-1}$  at 50°N.

Poleward of 20°S and 30°N the heat equation for the temperature  $T$  gains a term  $\gamma(T - T^*)$ , where  $T^*$  is the prescribed monthly mean climatological temperature for the region under consideration, and  $\gamma$  is a Newtonian cooling coefficient. Its value is  $1/(2 \text{ days})$  near the zonal boundaries and decreases to a value of zero equatorward of 30°N

and  $20^{\circ}\text{S}$ . This device mitigates the effect of the artificial zonal walls along the southern and northern boundaries of the ocean and forces the solution towards the climatology in these regions. There are similar terms in the horizontal momentum equations.

The heat flux across the ocean surface is:

$$Q = SW - LW - QS - QE$$

The solar short wave heating  $SW$  is taken to be 500 ly per day equatorward of  $20^{\circ}$  latitude and decreases linearly to 300 ly per day between  $20^{\circ}$  and  $45^{\circ}$  latitude. The long wave back radiation  $LW$  has the constant value of 115 ly per day. The sensible heat flux is:

$$QS = \rho C_D C_p V (T_0 - T_A)$$

and the evaporation is:

$$QE = \rho C_g L V [\exp(T_0) - \gamma \exp(T_A)] (0.622/p)$$

Here  $\rho = 1.2 \times 10^{-3} \text{ g cm}^{-3}$ ;  $L = 595 \text{ cal g}^{-1}$ ;  $C_D = 1.4 \times 10^{-3}$ ;  $p = 1013 \text{ mb}$ ;  $C_p = 0.24 \text{ cal g}^{-1} \text{ }^{\circ}\text{C}^{-1}$ ;  $T_0$  is the sea-surface temperature in degrees Kelvin;  $T_A$  is the atmospheric temperature at the surface;  $V$  is the surface wind speed; and the relative humidity  $\gamma$  is assigned the constant value 0.8. No provision is made for clouds. The sensible heat flux is found to be of secondary importance so that variations in heat flux are primarily a consequence of change in the evaporation. For the El Niño simulations the atmospheric temperature  $T_A$  is assumed to be  $1^{\circ}\text{C}$  less than the predicted sea-surface temperatures. The results to be shown are for this value. The sea-surface temperatures are found to be unrealistically high and can exceed  $32^{\circ}\text{C}$ . An experiment in which  $T_0 - T_A = 2^{\circ}\text{C}$  gives exactly the same sea-surface temperature patterns except that the values of the contours are  $3^{\circ}\text{C}$  less. This suggests that  $T_0 - T_A = 1.5^{\circ}\text{C}$  would have been the best parameterization. Fields other than sea-surface temperature were unaffected by the change in the value for  $T_0 - T_A$ . Since evaporation depends on the wind speed, avoidance of excessively high temperatures in regions of weak winds required that the wind speed not be less than  $4.8 \text{ m s}^{-1}$ . This minimum parameterizes evaporation caused by high-frequency wind fluctuations that are absent from the mean monthly winds.

The initial conditions for the model are zero currents and the climatological temperature field (Levitus, 1982). Month averaged climatological winds then force the model for three years by which time the model has an equilibrium seasonal cycle. After this stage the model was forced with monthly mean winds for 1982 and 1983, provided by the National Meteorological Center.

There are several reasons for expecting discrepancies between the results from this model and the measurements. The parameterization of sub-grid scale mixing processes, the artificial zonal boundaries along the northern and southern extremes of the basin, the absence of all islands, including the Galapagos, and the incorrect initial conditions — conditions in January 1982 differed from those in the model at that time — all contribute to the errors. Probably of most importance are errors in the surface boundary conditions, especially the surface winds which were available on a very coarse spatial and temporal grid. In spite of these handicaps, the model performed surprisingly well. Changes in the heat content of the ocean, a variable that is correlated with sea level, are in good agreement with the measurements in Fig. 4. It can be argued that this is not a severe test for

the model because the heat content, being a (vertical) integral, is a relatively simple variable and can readily be simulated with linear one-level models (Busalacchi and O'Brien, 1981). Simulation of changes in the vertical structure of the flow is a more stringent test for the model. Figures 8 and 9 demonstrate the ability of the model to reproduce such changes on the equator at  $160^{\circ}$  and  $95^{\circ}\text{W}$ . The considerable differences in the variability at these locations (Figs. 5 and 6), to be discussed in more detail later, are reproduced fairly well. [Keep in mind that spatial gradients are large near  $0^{\circ}\text{N } 95^{\circ}\text{W}$  which is close to the Galapagos Islands (at  $0^{\circ}\text{N } 90^{\circ}\text{W}$ ).] Serious flaws appear in the model primarily towards the end of 1983 when isotherms fail to rise to the surface at  $0^{\circ}\text{N } 95^{\circ}\text{W}$ , for example. Comparison with measurements in other regions reveal that the simulation of the recovery from El Niño after July 1983 was in general poor in all parts of the tropical Pacific Ocean. The following discussion of results is therefore limited to the period through July 1983. The extent to which errors in the wind field caused the discrepancies between the measurements and the model will be assessed once better wind data are available.

#### 4. RESULTS

Figure 10 shows the simulated surface currents at various states of El Niño. Advection by these currents altered the sea-surface temperature patterns as shown in Fig. 11, and redistributed the warm waters of the upper ocean as shown in Fig. 12. By July 1982, there was intense eastward flow in the western equatorial Pacific while the southeast trades maintained westward flow in the eastern equatorial Pacific. During the subsequent months the region of unusual eastward flow expanded latitudinally – the region extends from  $9^{\circ}\text{S}$  to  $9^{\circ}\text{N}$  approximately – and eastward. The persistence of the southeast trade-winds inhibited the eastward flow at and south of the equator from penetrating much beyond  $120^{\circ}\text{W}$  by November 1982, but the North Equatorial Countercurrent had reached the coast of Central America by that time. This intensified the anti-clockwise circulation around the Costa Rica Dome (Fig. 12), a feature observed by Barberan et al. (1984) and also resulted in the southward advection of warm surface waters across the equator in the region east of the Galapagos Islands (Figs. 13 and 11). The increase in the heat content of the eastern tropical Pacific after July 1982 was at the expense of the off-equatorial regions to the west of the dateline where the thermocline shoaled (Fig. 12).

Figure 14 shows the development of the surface and subsurface flow along the equator. The eastward winds west of the dateline between July and November 1982 (Fig. 1) are seen to drive intense eastward surface jets in the ocean. The jet of November 1982 is exceptionally intense and penetrates far east. It was this one that Firing et al. (1983) observed at  $159^{\circ}\text{W}$  (Fig. 5). Below the surface the Equatorial Undercurrent decelerated steadily after July 1982. This happened because the zonal pressure gradient that drives this current decreased steadily as more and more warm surface water was advected eastward (Fig. 15). By November 1982 the slope of the thermocline to the west of  $160^{\circ}\text{W}$  had actually reversed (Fig. 16).

The changes during the first phase of El Niño, up to December 1982, are in response to the relaxation of the tradewinds. Studies of the response to idealized changes in the wind indicate that the time-scale that characterizes the wind variations is a very important



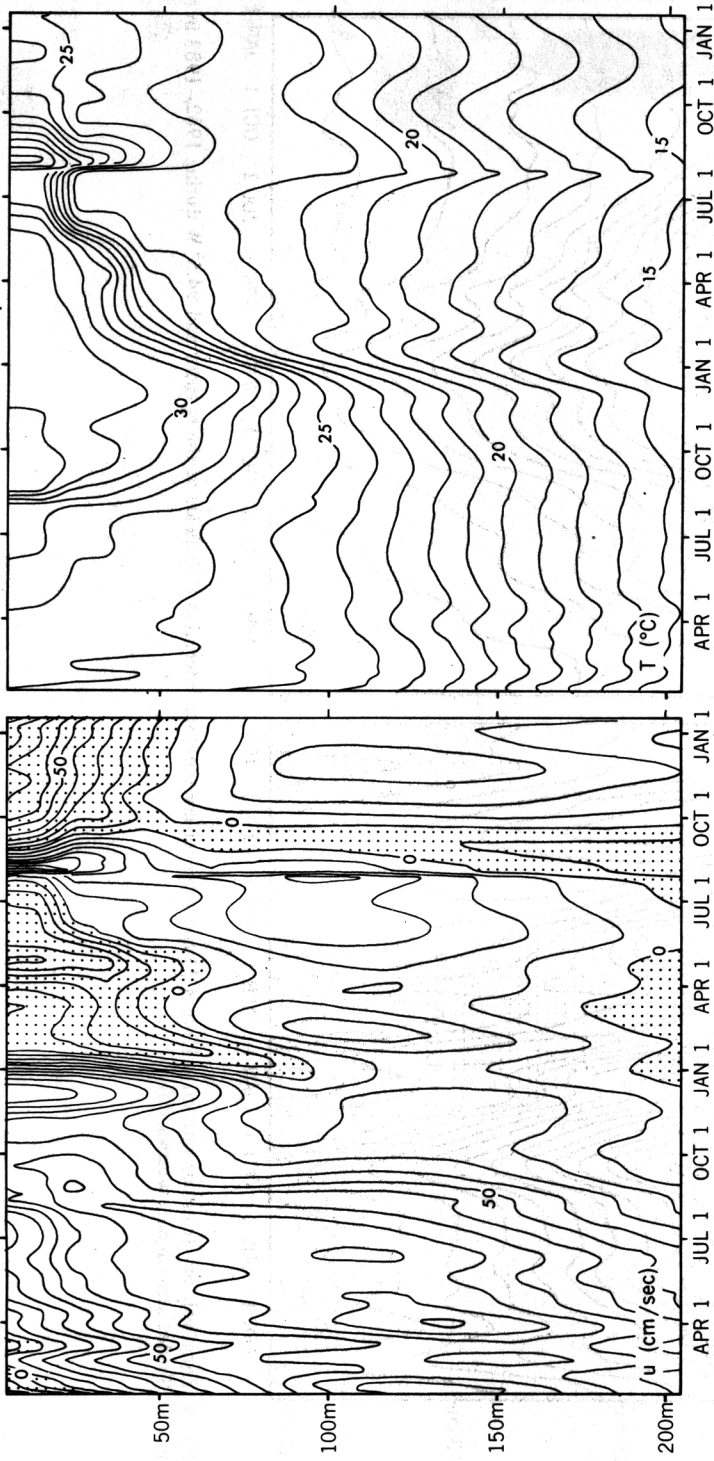


Fig. 8. Zonal velocity (contour interval =  $10 \text{ cm s}^{-1}$ ) and temperature (contour interval =  $1^{\circ}\text{C}$ ) fields at the equator and  $159.5^{\circ}\text{W}$  during 1982–1983 in the model. Shaded areas denote westward flow.

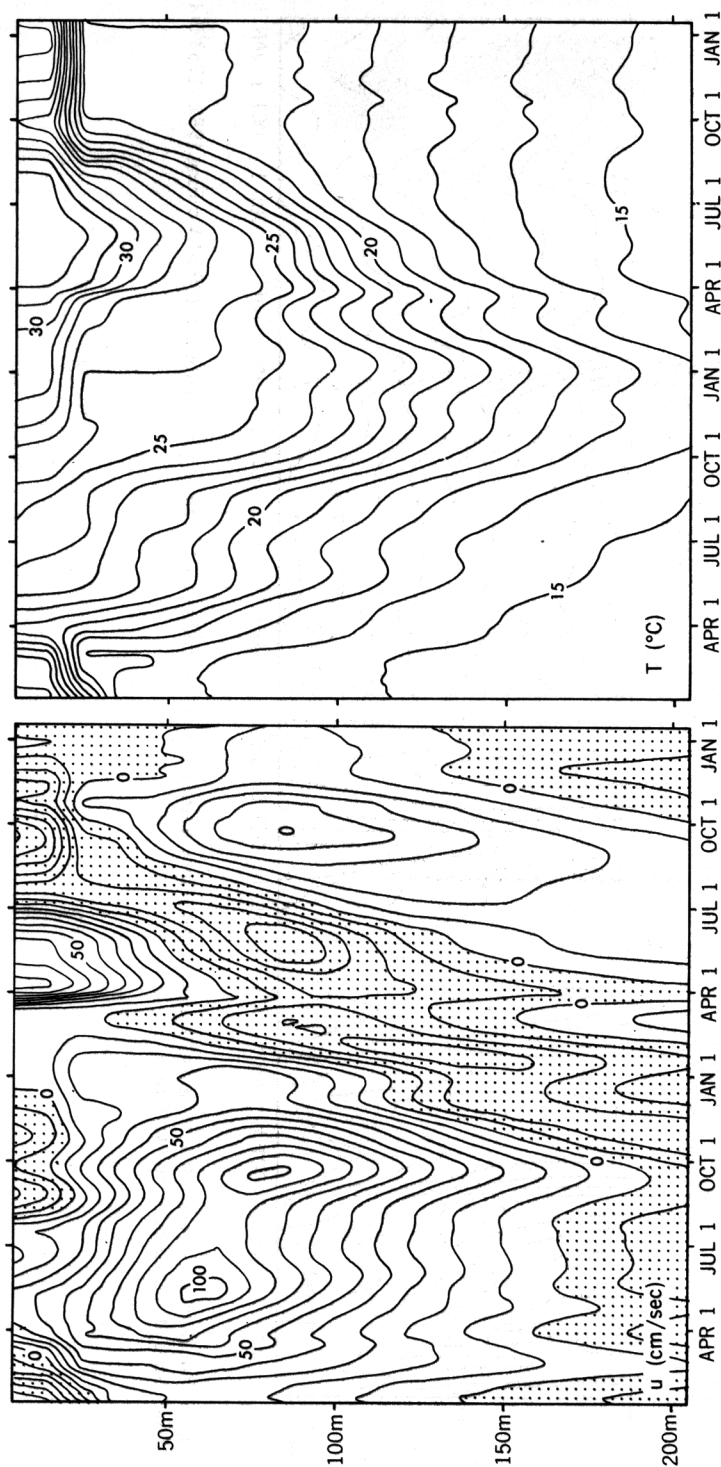


Fig. 9. Zonal velocity (contour interval =  $10 \text{ cm s}^{-1}$ ) and temperature (contour interval =  $1^{\circ}\text{C}$ ) fields at the equator and  $94.5^{\circ}\text{W}$  during 1982–1983 in the model. Shaded areas denote westward flow.

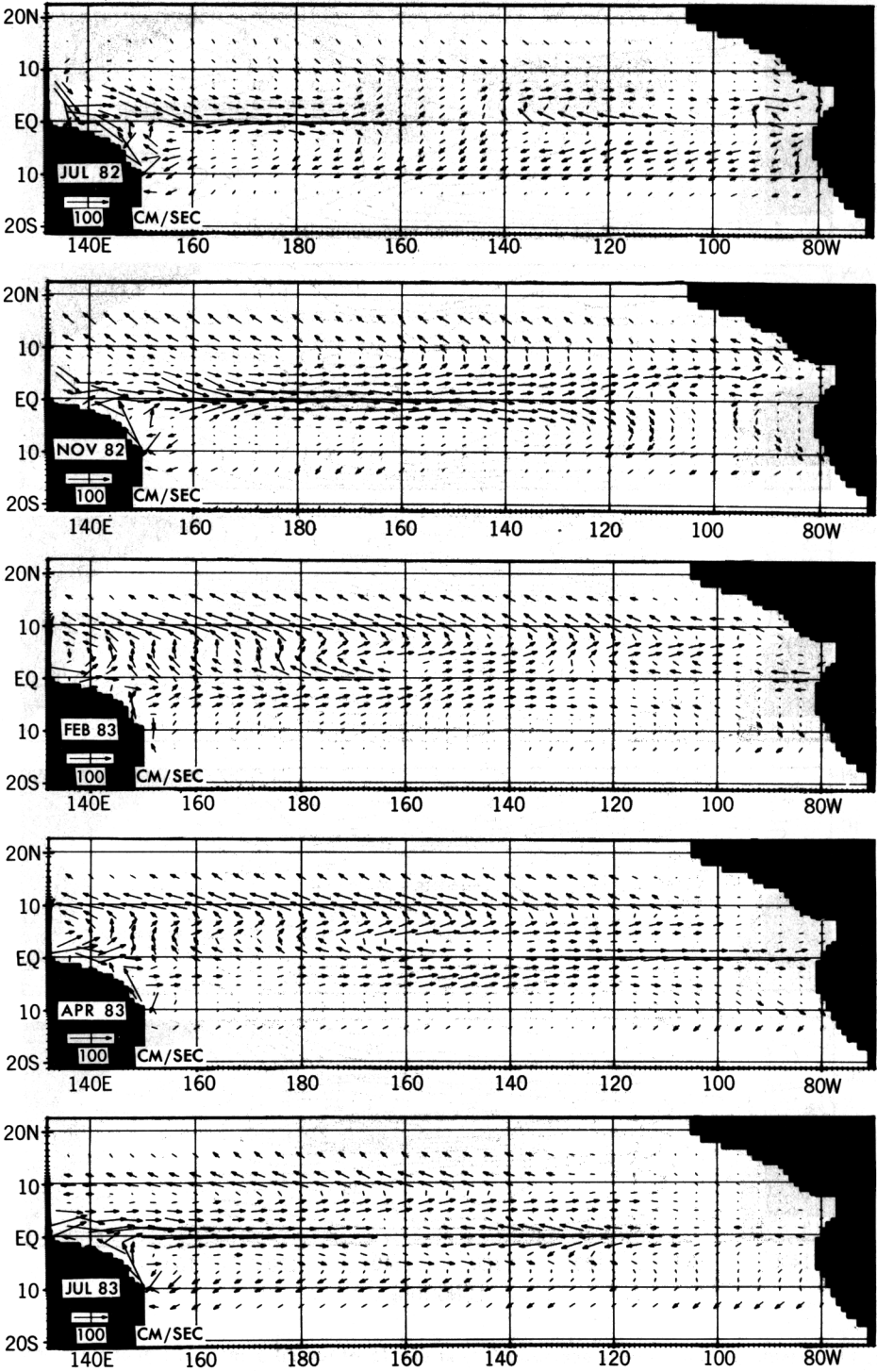


Fig. 10. Horizontal velocity vectors at a depth of 5 m. These are instantaneous values at day 15 of the indicated months.

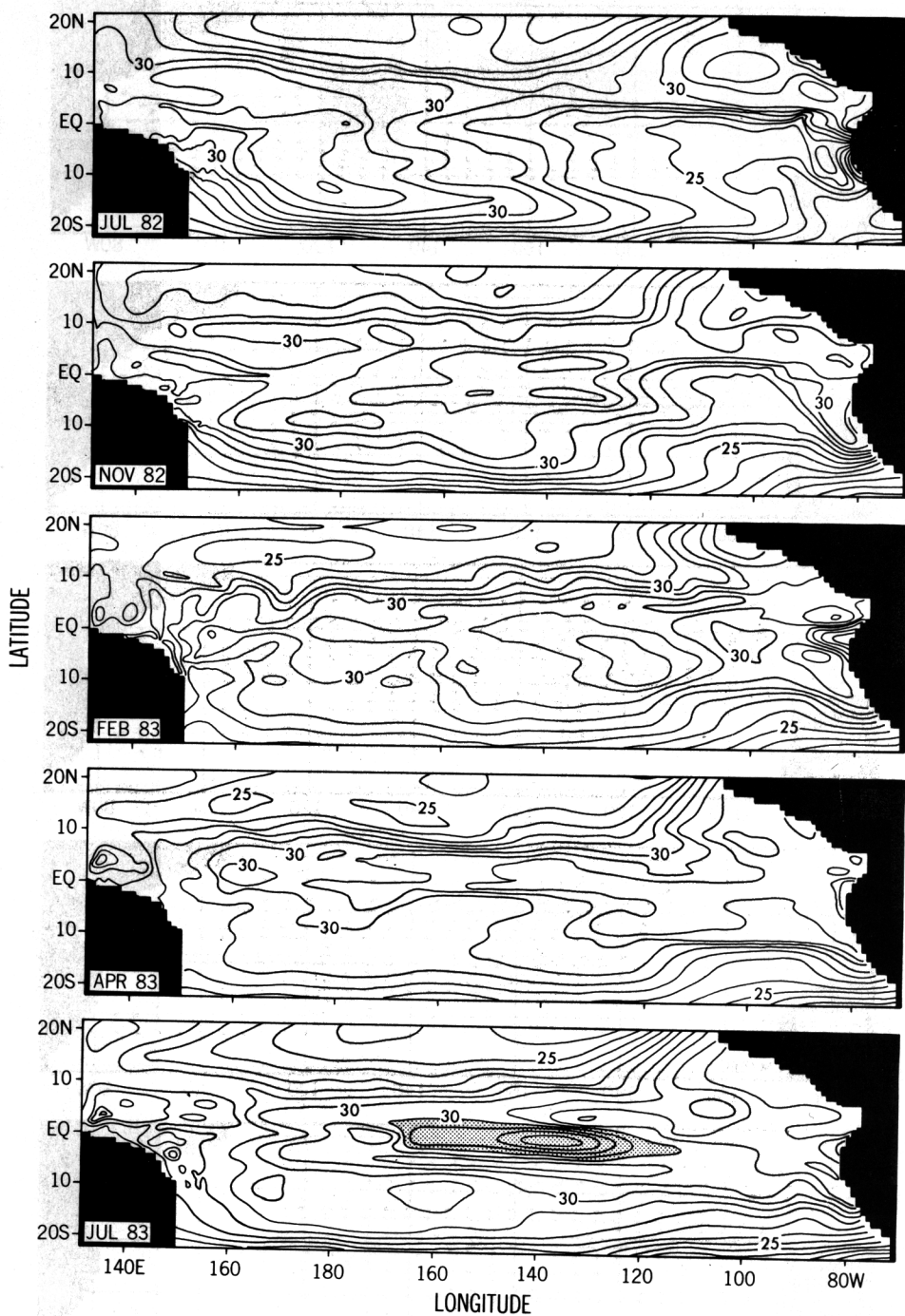


Fig. 11. Instantaneous maps of temperature ( $^{\circ}\text{C}$ ) at day 15 of several months at 5 m depth. Contour interval is  $1^{\circ}\text{C}$ . In the map for July 1983 the temperature in the shaded equatorial region is less than  $30^{\circ}\text{C}$ .

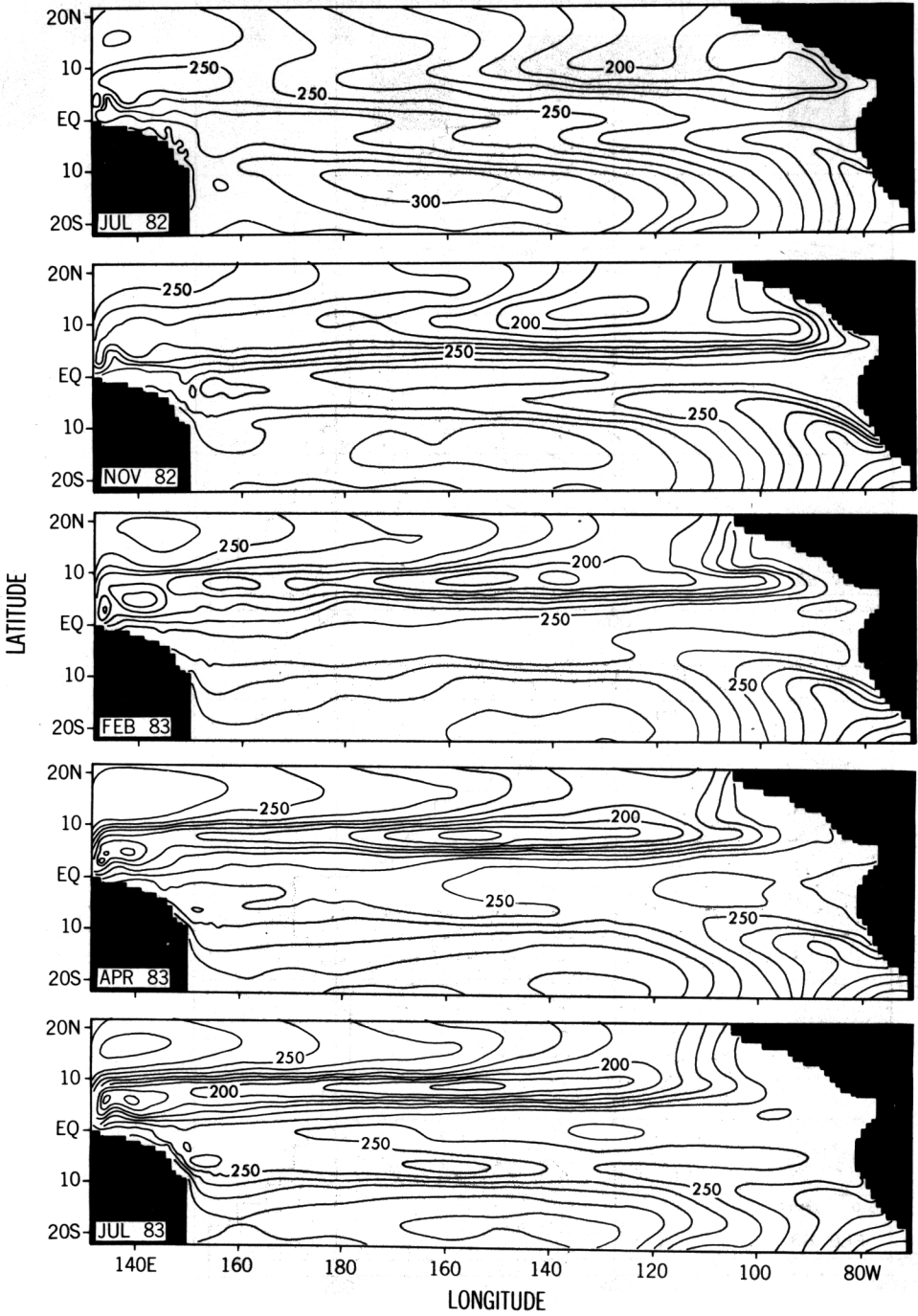


Fig. 12. Heat storage maps integrated to a depth of 317 m. Contour interval is  $1.0 \times 10^{-5} \text{ J cm}^{-2}$ .

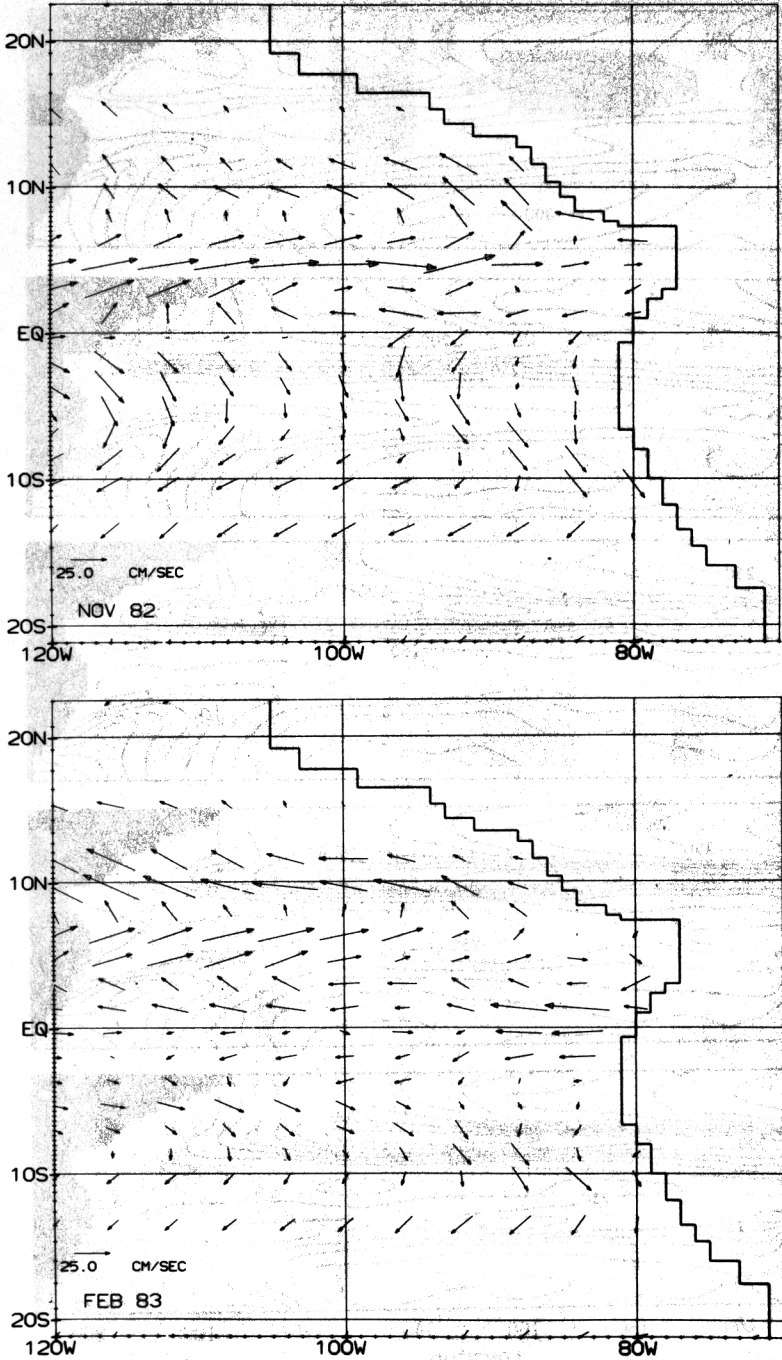


Fig. 13. Horizontal velocity vectors for November 1982 and February 1983 shown on a larger scale than Fig. 10 for the eastern Pacific.



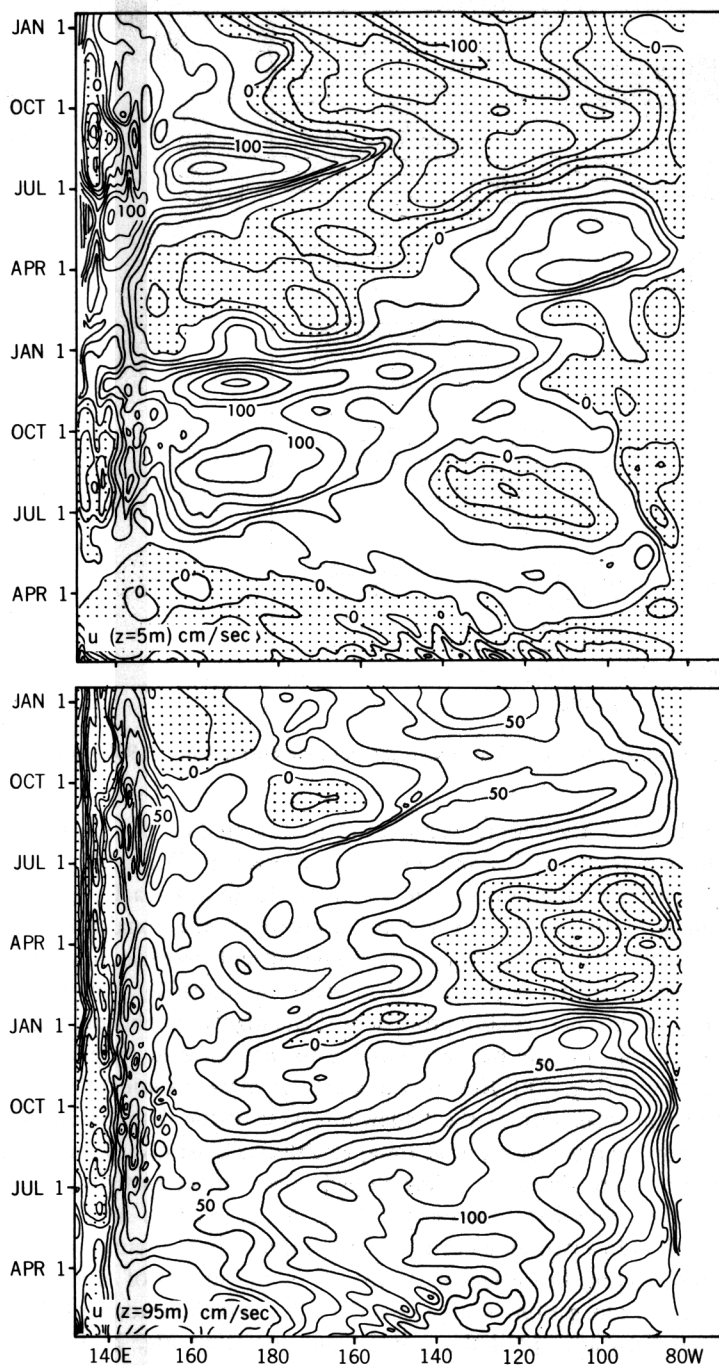


Fig. 14. Zonal velocity along the equator for 1982–1983 at 5 m (contour interval = 20 cm s<sup>-1</sup>) and 95 m (contour interval = 10 cm s<sup>-1</sup>). Westward flow is shaded.

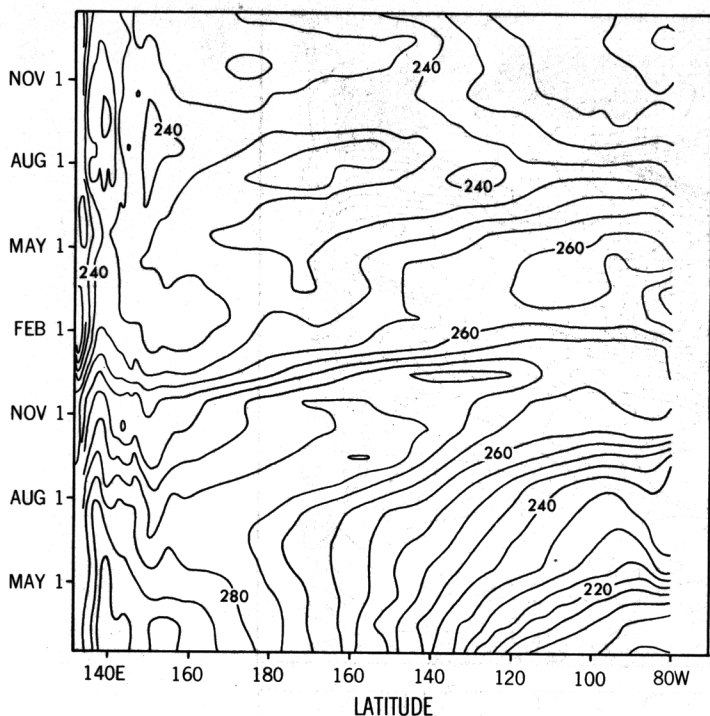


Fig. 15. Vertically integrated heat storage (to 317m) along the equator during 1982–1983. Contour interval is  $5.0 \times 10^4 \text{ J cm}^{-2}$ .

factor (Philander, 1981). In 1982 there were examples of both a gradual change in the winds (between June and November 1982) and an abrupt change, in December 1982 (Fig. 1). The response to a gradual change is one in which the ocean is at each moment practically in equilibrium with the wind. The gradual decrease of the zonal pressure gradient and the gradual deceleration of the Equatorial Undercurrent between June and November 1982 are examples of such a response. Kelvin waves undoubtedly play a role during this period, but they are not particularly prominent. [The highly variable eastward phase propagation evident in Fig. 14 is in part attributable to the eastward propagation of the weakening of the trades (Fig. 1).] Kelvin waves are far more prominent in the oceanic response to the abrupt relaxation of the tradewinds west of the dateline during December 1982. The eastward winds had, by that time, established a westward pressure force in the western Pacific where the thermocline sloped down to the east (Fig. 16). The abrupt relaxation of the winds left this pressure force unbalanced. It accelerated the surface waters westward and caused an elevation of the thermocline. Figures 14 and 15 show Kelvin waves propagating this effect eastward, as in the model of McCreary (1976). The eastward phase propagation is at a speed in the neighbourhood of  $160 \text{ cm s}^{-1}$ , considerably faster than any speed that can be inferred from Fig. 14 for the months before December 1982. This speed implies an equivalent depth of 25 cm, a value close to that of the second baroclinic mode. However, inspection of the vertical structure of the flow reveals that far more than a single vertical mode was involved. The abrupt rise of the thermocline in December 1982 affected the ocean at  $160^\circ\text{W}$  from the surface

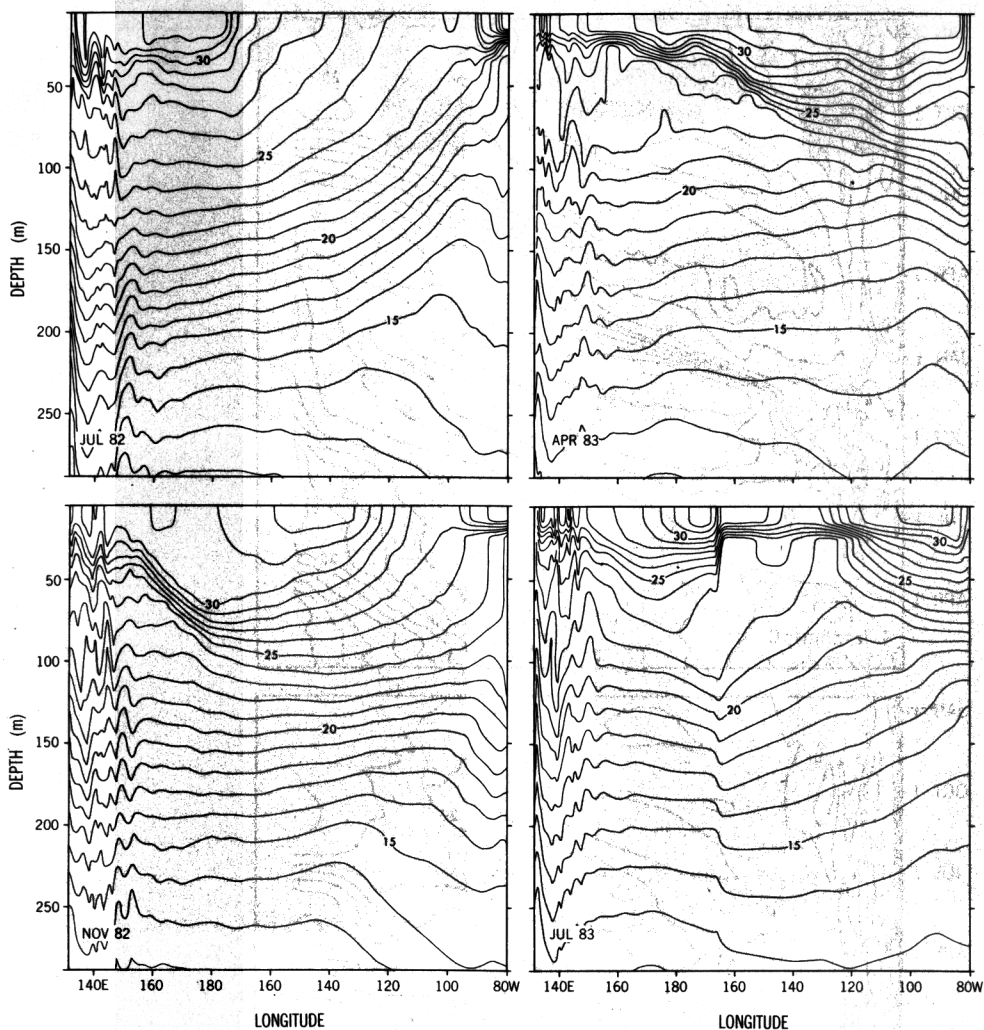


Fig. 16. Zonal sections of temperature ( $^{\circ}\text{C}$ ) along the equator on the 15th of several months.

to a depth of 200m at least (Fig. 8), but further east, at  $95^{\circ}\text{W}$ , the thermal field of the upper 75 m of the ocean was unaffected (Fig. 9). This suggests that the Kelvin wave excited in the western Pacific in early December 1982 travelled eastward *and* downward. This is confirmed by Fig. 17 which shows that, at a depth of 55 m the rise of the thermocline in December 1982 peters out in the neighbourhood of  $140^{\circ}\text{W}$ , but at a depth of 95 m this rise is evident much further east. Note that none of Figs. 14, 15 and 17 shows westward phase propagation that could suggest reflection of Kelvin waves off the South American coast. The reason presumably is that a downward propagating Kelvin wave reflects as a Rossby wave that continues to propagate further downward. In response to periodic forcing, there is relatively little vertical dispersion as beams travel eastward and downward (McCreary, 1984) but wind pulses, such as that of November 1982 will cause considerable vertical dispersion. This interesting topic will be pursued on another

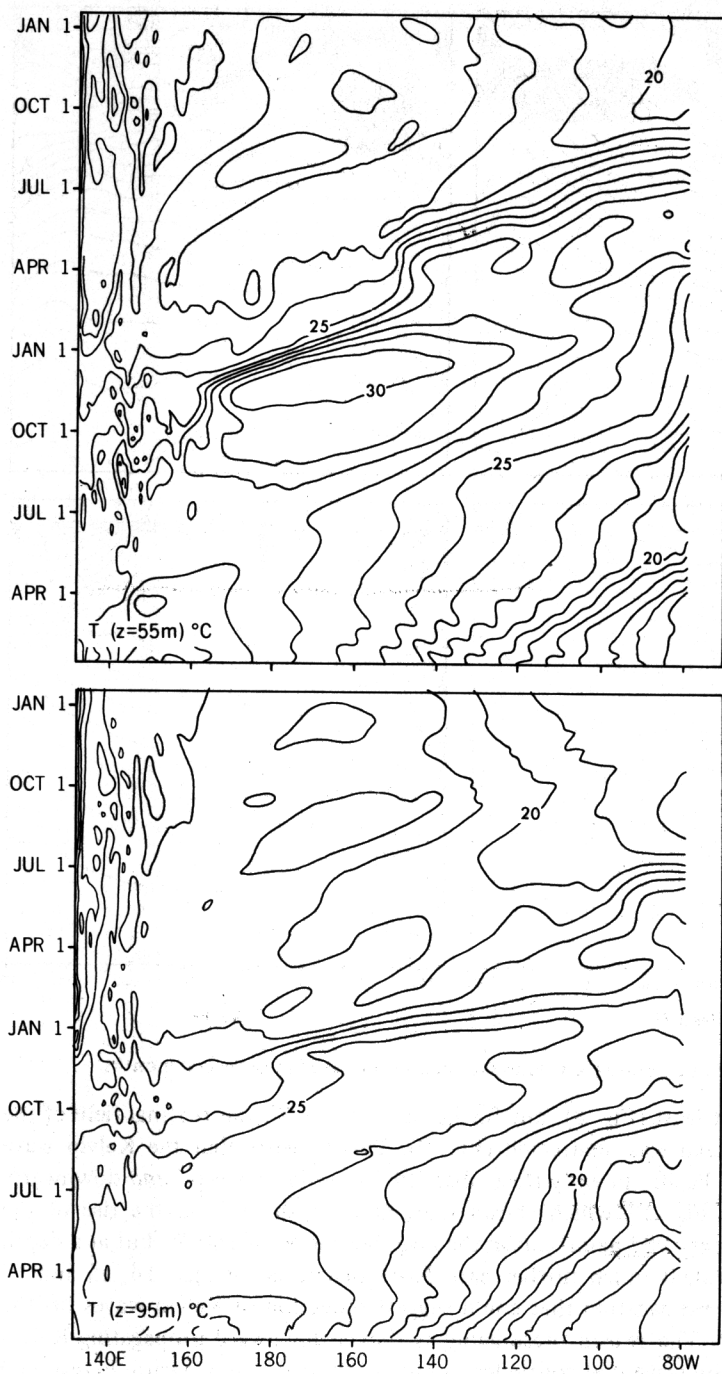


Fig. 17. Temperatures at 55 and 95 m during 1982–1983 along the equator.

occasion. Here, we note that one-level models that ignore the continuous stratification of the ocean could greatly exaggerate the importance of reflected waves on the upper ocean.

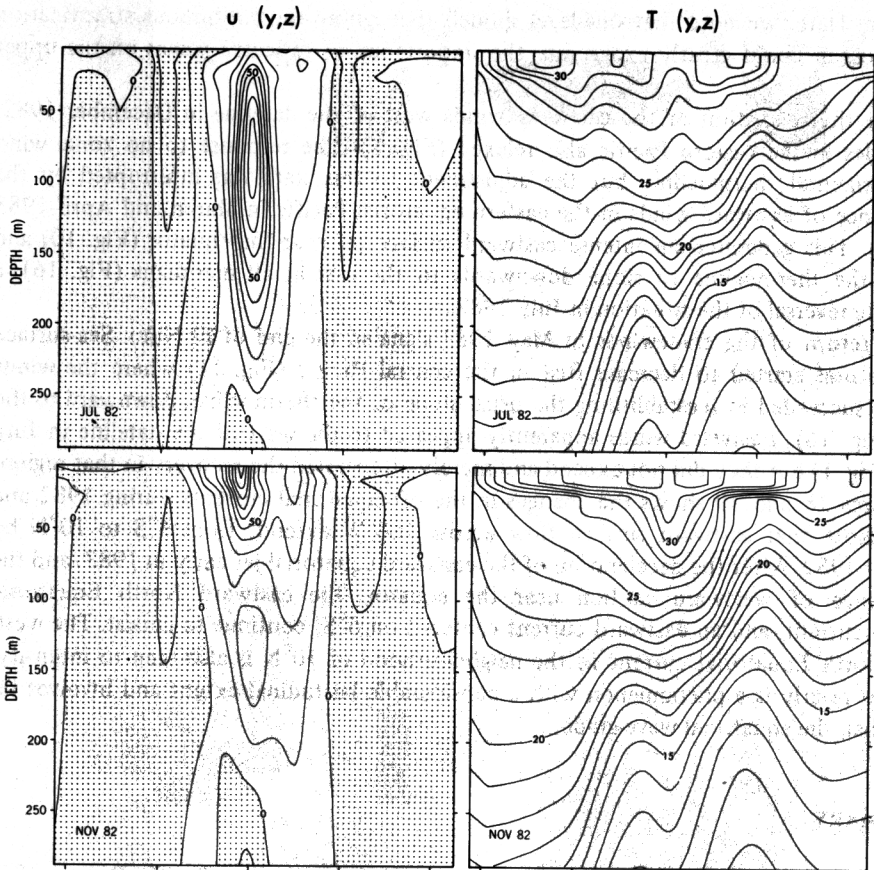
After the relaxation of the eastward winds west of the dateline in December 1982, the trades in the eastern Pacific also relaxed (Fig. 1). The response to no zonal wind is a horizontal thermocline, but the adjustment to this state was interrupted by the appearance of eastward winds in the eastern equatorial Pacific in March and April 1983 (Fig. 1). This generated an intense eastward surface jet near the equator (Fig. 10) and caused the thermocline to slope downwards to the east at all meridians (Fig. 16), a complete reversal of the situation in July 1982.

The return of the tradewinds in May 1983 signaled the end of El Niño. Sea-surface temperatures started to decrease first in the central Pacific (Fig. 11) where the winds quickly succeeded in reestablishing the usual slope of the thermocline, downward to the west (Fig. 16). Eastward winds apparently appeared to the west of the dateline in July 1983 (Fig. 1) but they did not expand and merely interrupted the recovery in that region.

Figures 18 and 19 shows the changes in the off-equatorial currents during 1982 and 1983. Note that eastward surface flow across  $160^{\circ}\text{W}$  extends from  $6^{\circ}\text{S}$  to  $10^{\circ}\text{N}$  by October 1982. After the deceleration of the eastward equatorial jet early in 1983, and the appearance of westward motion near the equator, the eastward North Equatorial Countercurrent, and an eastward current centered on  $6^{\circ}\text{S}$ , continue to persist. The westward North Equatorial current in the neighbourhood of  $10^{\circ}\text{N}$  is also seen to intensify. El Niño clearly is a phenomenon with a considerable latitudinal extent and involves far more than the equatorial wave-guide.

## 5. SUMMARY

A simulation, with a general circulation model of the tropical Pacific Ocean, of El Niño of 1982–1983 succeeds reasonably well in reproducing the few available measurements. This establishes confidence in the results in regions where measurements are unavailable. The model shows that the eastward transfer of heat from the western to the eastern tropical Pacific was affected by unusual eastward surface currents which, by November 1982, extended from  $9^{\circ}\text{S}$  to  $9^{\circ}\text{N}$  across  $120^{\circ}\text{W}$ . Further east the persistence of the southeast tradewinds inhibited eastward surface flow at and to the south of the equator at that time, but the eastward North Equatorial Countercurrent between  $3^{\circ}$  and  $8^{\circ}\text{N}$  penetrated right to the coast of Central America. The intensification of the North Equatorial Countercurrent affected the sea-surface temperature field significantly (Fig. 11), especially to the east of the Galapagos Islands where warm surface waters flowed southward across the equator. The pattern of changes in the heat content of the upper 300 m of the ocean (Fig. 12) differs from that of the sea-surface temperature and reflects the importance of the equatorial wave-guide where there were oceanic changes to a considerable depth. The oceanic response to the gradual relaxation of the trade winds between June and November 1982 was approximately an equilibrium so that the zonal pressure gradient, which the trades had maintained, and the intensity of the Equatorial Undercurrent, which the pressure gradient had maintained, decreased with the winds.



By the end of 1982, eastward winds had reversed the sign of the pressure gradient and eliminated the Equatorial Undercurrent (Fig. 14). Kelvin waves undoubtedly played a role in the adjustment of the ocean to the weakening of the trades, but they were not particularly prominent until December 1982. An abrupt weakening of eastward winds to the west of the dateline during that month caused a rapid rise of the thermocline and a westward acceleration of the surface currents right across the equatorial Pacific Ocean (Figs. 14 and 15). The Kelvin waves that induced these changes dispersed downward while propagating eastward. Waves excited by reflection at the coast of South America apparently continued to propagate downwards because there is no evidence of such reflected waves affecting the upper ocean.

The initial recovery from El Niño in early 1983 was interrupted by the appearance of eastward winds near the equator in the eastern half of the basin in March and April 1983 (Fig. 1). By this time the slope of the thermocline all along the equator, was downwards to the east, the opposite of what it had been in July 1982 (Fig. 16). The return of the tradewinds in May 1982 signalled the end of El Niño. A fall in sea-surface temperatures and reestablishment of the normal slope of the thermocline first occurred in the central equatorial Pacific Ocean.



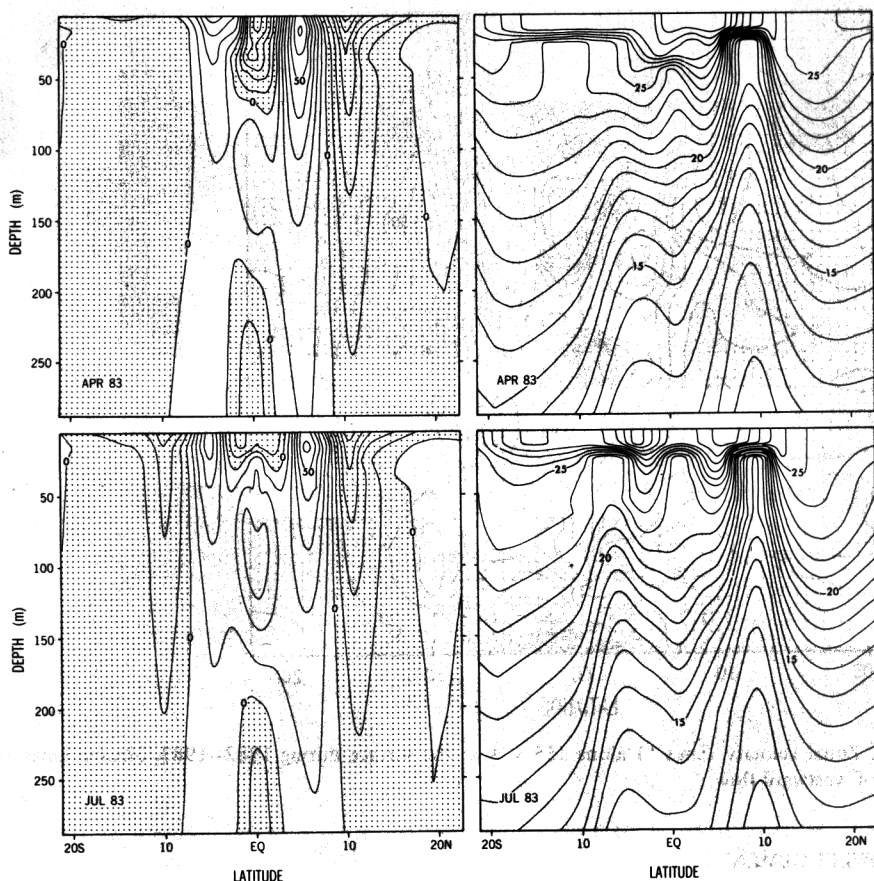


Fig. 18. Meridional sections of zonal velocity and temperature along 159.5W on the 15th of different months. Contour intervals are  $1^{\circ}\text{C}$  and  $10\text{ cm s}^{-1}$ , respectively. Shaded regions indicate westward flow.

The success of the model is surprising because it is widely believed (as stated earlier) that the winds that drive the model are not very accurate. The monthly mean winds suppress information about high-frequency fluctuations. Such fluctuations must have caused the abrupt changes in sea level that were seen at Christmas Island in July 1982 (Fig. 4) but which are absent from the model. The grid of  $5^{\circ}$  longitude by  $5^{\circ}$  latitude on which the data are available precludes accurate estimates of the curl of the wind which must have been an important factor in the intensification of the off-equatorial currents. Time-series measurements of the winds at  $0^{\circ}\text{N } 110^{\circ}\text{W}$  and  $0^{\circ}\text{N } 95^{\circ}\text{W}$  (Halpern, 1984) suggest that the region of considerable wind variations during 1982 did not extend as far eastward as is shown in Fig. 1. Given the inaccuracies in the wind field, it is premature to make a detailed comparison between the results from the model and the measurements. Such comparisons, and more detailed analyses of the model results, will be made once the calculations have been repeated with an improved wind data set.

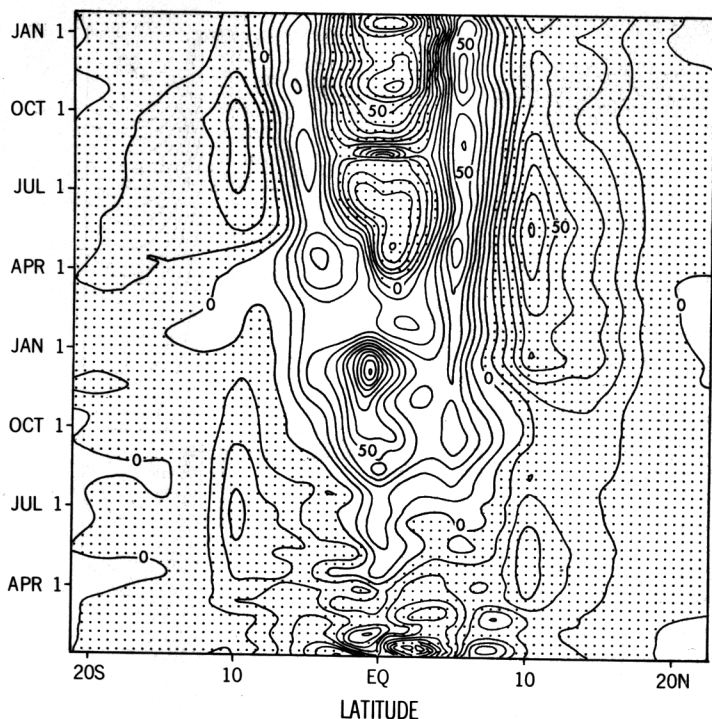


Fig. 19. Zonal velocity ( $\text{cm s}^{-1}$ ) along  $155.5^\circ\text{W}$  at the surface during 1982–1983. Shaded areas are regions of westward flow.

#### ACKNOWLEDGEMENTS

We are indebted to D. Hansen for valuable comments on an earlier draft of the manuscript, to R. Pacanowski for assistance with the computations, and to P. Tunison and J. Pege for assistance in the preparation of the paper.

#### REFERENCES

- Barberan, J., Gallegus, A. and Padilla, A., 1984. The Costa Rica Dome during the onset of the 1982–1983 El Niño. *Trop. Ocean–Atmos. Newsl.*, 24: 13–14.
- Bryan, K., 1969. A numerical method for the study of the world ocean. *J. Comput. Phys.*, 4: 347–376.
- Busalacchi, A.J. and O'Brien, J.J., 1981. Interannual variability of the equatorial Pacific in the 1960's. *J. Geophys. Res.*, 86: 10901–10907.
- Firing, E., Lukas, R., Sades, J. and Wyrski, K., 1983. Equatorial undercurrent disappears during 1982–1983 El Niño. *Science*, 222: 1121–1123.
- Halpern, D., 1984. Upper ocean current and temperature observations along the equator west of the Galapagos Islands before and during the 1982–83 ENSO event. *El Niño/Southern Oscillation Workshop, Climate Res. Comm., Natl. Res. Counc., Miami, Fla.*
- Hansen, D., 1984. Surface drifter measurements in the eastern equatorial Pacific during El Niño of 1982–1983. (In prep.)

- Katz, E.J., 1984. Basin wide thermocline displacements along the equator of the Atlantic in 1983. *Geophys. Res. Lett.*, 11: 729-732.
- Levitus, S., 1982. Climatological atlas of the world ocean. NOAA Prof. Pap. 13, 173 pp., U.S. Govt. Printing Office, Washington, D.C.
- McCreary, J.P., 1976. Eastern tropical ocean response to changing wind systems: with application to El Niño. *J. Phys. Oceanogr.*, 6: 632-645.
- McCreary, J.P., 1984. Equatorial beams. *J. Mar. Res.*, 42: 395-430.
- Meyers, G. and Donguy, J.R., 1984. The North Equatorial Countercurrent and heat storage in the western Pacific Ocean during 1982-83. *Nature*, in press.
- Pacanowski, R. and Philander, S.G.H., 1981. Parameterization of vertical mixing in numerical models of tropical oceans. *J. Phys. Oceanogr.*, 11: 1443-1451.
- Philander, S.G.H., 1981. The response of equatorial oceans to a relaxation of the trade winds. *J. Phys. Oceanogr.*, 11: 176-189.
- Philander, S.G.H. and Pacanowski, R.C., 1984. Simulation of the seasonal cycle in the tropical Atlantic Ocean. *Geophys. Res. Lett.*, 11: 802-804.
- Wyrski, K., 1984a. Pacific-wide sea level fluctuations during the 1982-1983 El Niño. In: *Galapagos 1982-1983: A Chronicle of the Effects of El Niño*. Charles Darwin Research Station, Guayaquil, Ecuador, in press.
- Wyrski, K., 1984b. Monthly maps of sea level in the Pacific during El Niño of 1982 and 1983. In: *Time Series of Ocean Measurements*, Vol. 2. I.O.C. Tech. Ser. No. 25, UNESCO, Paris.